RSC Advances

PAPER

View Article Online
View Journal | View Issue

Cite this: *RSC Adv.*, 2026, **16**, 19870

Integrated sonication-assisted deep eutectic solvent for extraction of antibacterial compounds from cacao shells

Yuni Kusumastuti, *[ab] Jordan Maulana Ma'arif,[b] Muh. Irsal,[b] Dewanti Cahya Widi, [bc] Nur Rofiqoh Eviana Putri, [ab] Mukmin Sapto Pamungkas, [ab] Lusiana Olivia[b] and Jonas Kristanto[a]

The valorization of cacao shells offers high added value because of the rich content of bioactive compounds. This study investigated the application of cacao shell waste as an antibacterial agent through green extraction processes. The extraction was carried out by integrating SAE-DES (sonication-assisted and deep eutectic solvent) with a choline chloride-lactic acid-based solvent. The parameters of extraction, including temperature, solid-to-solvent ratio, and DES concentration, were optimized applying a Box–Behnken design in RSM (response surface methodology). The optimum conditions were found to be 80 °C, a solid-to-solvent ratio of 1 : 10, and a DES concentration of 62.65%, with TPC (total phenolic content) and TFC (total flavonoid content) of 4.94 ± 0.10 g GAE per g sample and 5.97 ± 0.09 g RE per g sample, respectively. Additionally, the mass transfer coefficient ($k_c a$) and equilibrium constant (H_s) range from 8.73 × 10^{-3} to 14.80 × 10^{-3} min^{-1} and 0.56 × 10^{-3} to 41.91 × 10^{-3} g solid per cm^3, respectively. FTIR analysis confirmed the presence of significant functional groups of phenolic compounds in the extract. Furthermore, the extract was effective against *Escherichia coli* and *Staphylococcus aureus*.

Received 27th February 2026
Accepted 2nd April 2026

DOI: 10.1039/d6ra01724j

rsc.li/rsc-advances

1 Introduction

Agro-industrial waste management through valorization strategies is an important step toward supporting the circular bioeconomy, as it can convert biomass waste into high-value products.[1] One type of agro-industrial waste that is abundant but underutilized is cacao shells. As a significant by-product of the chocolate industry, cacao shells account for approximately 80% of total cacao fruits biomass.[2] However, accumulated cacao shell waste is often disposed of without further processing, causing environmental problems such as unpleasant odors and becoming a breeding ground for pests and pathogens that significantly reduce plantation productivity.[3] Although they have been used as animal feed, the utilization of cacao shells is still constrained by *Theobromine* content, which can inhibit animal growth and disrupt rumen microbial activity.[4] Therefore, alternative methods are needed to explore the benefits of cacao shells.

Cacao shells contain various bioactive compounds, including polyphenols, flavonoids (catechins, quercetin, epicatechins), phenolic acids (gallic acid, coumaric acid, and protocatechuic acid), and lignin derivatives.[5,6] These compounds have antioxidant, anti-inflammatory, and antimicrobial activities,[7,8] making cacao shells potentially useful in the development of biodegradable packaging materials,[9,10] natural food additives,[11] and nutraceutical products.[12] However, the cacao shells extraction is still a challenge due to their complex lignocellulose structure that inhibits the penetration of solvents and mass transfer. Cacao shells consist of the epithelial layer, mesocarp, and endocarp, which comprise a biopolymer matrix. The composition of the matrix consists of cellulose (44.69%), hemicellulose (11.15%), lignin (34.82%), and pectin (10.10%).[13] Therefore, the efficiency and quality of the compounds obtained are extremely dependent on the extraction methods, the solvents, and the operating conditions.

Extraction of phenolic compounds from cacao shells is generally carried out using conventional techniques including maceration and Soxhlet extraction with organic solvents like ethanol and methanol.[14] These methods are associated with certain drawbacks, including a lengthy extraction period, excessive use of solvents, as well as health and environmental risks. The harsh conditions of the process can lead to the degradation of sensitive compounds, causing low-yield extracts with reduced biological activity. Moreover, the observed

[a]*Chemical Engineering Department, Faculty of Engineering, Universitas Gadjah Mada, Jalan Grafika 2, Yogyakarta 55284, Indonesia. E-mail: yuni_kusumastuti@ugm.ac.id*
[b]*Smart Biomaterial Research Group, Chemical Engineering Department, Faculty of Engineering, Universitas Gadjah Mada, Jalan Grafika 2, Yogyakarta 55284, Indonesia*
[c]*Agrotropica Learning Center, Faculty of Agriculture, Universitas Gadjah Mada, Jalan Flora, Yogyakarta 55281, Indonesia*

limitations have led to the development of alternative environmentally friendly extraction methods, such as PLE (pressure liquid extraction), SAE (sonicated assisted extraction), SFE (supercritical fluid extraction), EAE (enzyme-assisted Extraction), LGE (liquid gas extraction), and MAE (microwave-assisted extraction).[15–17] The alternative techniques have been reported to enhance the extraction efficiency, lower the usage of solvent, and generate better reproducibility.[18,19] Among these methods, SAE is among the most efficient because it uses acoustic cavitation to break down the rigid plant cell matrix, thereby increasing solvent penetration and mass transfer.[20] However, SAE performance is strongly influenced by the solvent type, so selecting an appropriate solvent system remains a key factor for maximizing bioactive compound yield.

One type of solvent that is increasingly being developed is a DES (deep eutectic solvent), formed by combining HBA (hydrogen bond acceptors) and HBD (hydrogen bond donors). DES offers various advantages, including biodegradability, non-toxicity, and low volatility, making it more environmentally friendly.[21–23] In addition, organic acid-based DES have been reported to have intrinsic antimicrobial activity.[24] However, its high viscosity often limits mass transfer and extraction kinetics. Combining DES with SAE can overcome these limits by increasing compound diffusion. Nevertheless, the application of SAE–DES combinations to extract bioactive compounds such as TPC (total phenolic content) and TFC (total flavonoid content) from cacao shells remains very limited, offering opportunities for further research in optimizing the efficient, sustainable recovery of high-value compounds. Furthermore, achieving the highest and most optimum levels of these compounds is challenging because parameters like solvent concentration, temperature, and time often have complex interactions. Most previous analysis apply one factor at a time testing, which fails to show how these variables work together to affect the yield. Therefore, response surface methodology (RSM) is required to make a mathematical model that studies these interactions simultaneously to ensure an efficient, resource-saving, and high-quality extraction process.[25]

The analysis aims to maximize the green extraction of TPC and TFC from cacao shells applying an integrated SAE–DES method. To achieve this, RSM with a BBD (Box–Behnken design) was applied to assess the temperature interactions, solid–solvent ratio, and DES concentration. The obtained extracts were analyzed using the FTIR (Fourier Transform Infrared Spectroscopy), while the antibacterial efficacy was assessed against *Escherichia coli* and *Staphylococcus aureus* by the agar well diffusion technique. The findings provide a valuable contribution to the sustainable valorisation of cacao shell waste and the creation of natural antibacterial agents to be used in industries by searching for the best conditions to maximise yield with minimum resources imposed.

2 Materials and methods

2.1 Raw materials

Cacao shell waste, comprising Trinitario (75%) and Forastero (25%) varieties, was taken from the cacao plantation field in Pangandaran, West Java. The dried shells were milled with a laboratory grinder to produce the fine particles, followed by sieving with a Tyler mesh screen to obtain particles with mesh sizes ranging from −40 to +60.

Analytical grade reagents used in this study included ethanol p.a. (C_2H_6O, Supelco, ≥99.90%), sodium hydroxide p.a. (NaOH, Merck, ≥99.00%), aluminum chloride p.a. ($AlCl_3$, Merck, ≥98.00%), sodium nitrite p.a. ($NaNO_2$, Merck, ≥99.90%), gallic acid p.a. (Merck, 100.00%), rutin p.a. (Merck, ≥96.00%), sodium carbonate p.a. (Na_2CO_3, Merck, ≥99.90%), Folin–Ciocalteu reagent (Merck), choline chloride ($C_5H_{14}ClNO$, Himedia, ≥99.00%), lignin p.a. (Sigma-Aldrich, 95.00%), cellulose p.a. (Sigma-Aldrich, ≥99.90%), distilled water (aquadest), deionized water (aquabidest), and lactic acid ($C_3H_6O_3$. Himedia, ≥90.00%).

2.2 Deep eutectic solvent preparation

A DES was formulated by combining $C_5H_{14}ClNO$ and $C_3H_6O_3$ in a 1 : 2 molar ratio, following a modified procedure adapted from Xia *et al.*[26] A binary mixture of 100 g was stirred at 250 rpm for 2 h at 80 °C. The process continued until a clear, homogeneous, and uniform, indicating the complete formation of the eutectic phase.

2.3 Extraction and determination of the mass transfer constant

Solid–liquid extraction was performed by treating 5 g of dried cacao shell with the synthesized DES using ultrasonic-assisted extraction in an Elmasonic S30 (H). The experimental conditions were varied over a 40–80 °C temperature range, a solid-to-solvent ratio of 1 : 10–1 : 45 (w/v), and DES concentrations of 50–100% (v/v). During variation of each parameter, the other variables were kept constant at their default values (80 °C, 1 : 10 (w/v), and 100% (v/v)). Specifically, when temperature was varied, the solid-to-solvent ratio and DES concentration were fixed at 1 : 10 (w/v) and 100% (v/v), respectively. During the extraction, aliquots were collected at fixed time intervals from 5 to 240 minutes for mass transfer analysis. Each sample was subsequently diluted with ethanol before the analysis of TPC.

The mass transfer process was explained theoretically in three consecutive steps: (1) diffusion of phenolic compounds from the inside of the cacao shell matrix to the particle surface, (2) movement of solutes from the surface into the surrounding liquid film, and (3) convective transfer from the boundary layer into the bulk solvent medium. Among the proposed models, the convectively controlled mass transfer mechanism was considered most applicable in this study. This model considers that intra-particle diffusion occurs at a faster rate compared to interfacial transfer, as supported by the relatively small particle size and the rapid attainment of extraction equilibrium (within three hours).

$$N_A = k_c a\left(C^*_{Af} - C_{Af}\right) \quad (1)$$

Eqn (1) describes mass transfer based on Fick's law in convection, where N_A is the mass transfer rate of bioactive compounds from solids to solvent (g GAE per cm^3 min), $k_c a$ is the volumetric coefficient of mass transfer from solids to solvent (min^{-1}), and C^*_{Af} is the concentration of bioactive compounds at equilibrium with bioactive compounds in solids (g GAE per cm^3). C_{Af} is the concentration of bioactive compounds in the solvent (g GAE per cm^3). The equilibrium equation can be estimated by the formula as follows:

$$C^*_{Af} = H_s \times X_A \quad (2)$$

where H_s is the equilibrium constant (g solid per cm^3), and X_A is the concentration of bioactive compounds in the solid (g GAE per solid). The mass balance of bioactive compounds in the solvent is written as follows:

$$V\frac{dC_{Af}}{dt} = k_c a\left(C^*_{Af} - C_{Af}\right)V \quad (3)$$

$$V\frac{dC_{Af}}{dt} = k_c a\left(H_s \times X_A - C_{Af}\right)V \quad (4)$$

where V is the solvent volume (cm^3), for the mass balance of bioactive compounds in a solid, it can be written based on the following formula:

$$M_S\frac{dX_{Af}}{dt} = -k_c a\left(H_s \times X_A - C_{Af}\right)V \quad (5)$$

M_S is the mass of the extracted cacao shell solid (g solid). In addition the initial and boundary conditions in eqn (4) and (5) are:

$$t = 0 \times C_{Af} = C_{Af0} = 0 \times X_A = X_{A0} \quad (6)$$

$$t = t \times C_{Af} = C_{Af} \times X_A = X_A \quad (7)$$

The $k_c a$ and H_s parameters are evaluated based on the resulting R^2 coefficient (eqn (10)), which is desired to be high, close to 1. R^2 coefficient was obtained based on the SSE (sum of squared errors) and SST (total sum of squares), following:

$$SSE = \sum\left(C_{Af.calc} - C_{Af.data}\right)^2 \quad (8)$$

$$SST = \sum\left(C_{Af.data} - \overline{C}_{Af.data}\right)^2 \quad (9)$$

$$R^2 = 1 - \left(\frac{SSE}{SST}\right) \quad (10)$$

2.4 Extraction procedure and optimization using response surface methodology (RSM)

Solid–liquid extraction for optimization was performed using the same procedure as described for the mass transfer experiment, with experimental conditions based on those listed in Tables 1 and 2. The influence of SAE parameters on TPC and TFC recovery was statistically investigated through a BBD with three levels (−1, 0, and +1), as detailed in Table 1. The experiments totaled 15 randomized, including three replicates at the center point to ensure model accuracy and repeatability, as detailed in Table 2. Every extraction was conducted for 2.5 hours under specific operating conditions formulated by the experimental design. Following extraction, the obtained mixtures were centrifuged at 4000 rpm for 10 min to separate the supernatants from the solid residues. The supernatants and solid residues were collected and analyzed.

Table 1 Variables varied in SAE-DES extraction and the coded levels for the Box–Behnken design

		Coded levels		
Independent variables	Symbols	−1	0	1
Temperature (°C)	x_1	40	60	80
Ratio solid : solvent	x_2	1 : 10	1 : 25	1 : 40
DES concentration (% DES in water)	x_3	25	50	75

The RSM analyzes the main effects, interactions, and quadratic terms, which were then incorporated into a regression model to derive the predictive equation (eqn (11)).

$$Y = \beta_0 + \sum_{i=1}^{k}\beta_i x_i + \sum_{i=1}^{k}\beta_{ii}{x_1}^2 + \sum_{i=1}^{k}\sum_{j=1,\, j\neq i}^{k}\beta_{ij}x_i x_j + \varepsilon \quad (11)$$

where Y is the predicted response (TPC and TFC recovery), $x_1, x_2, \ldots, x_k$ represent the SAE-DES factors influencing the extraction efficiency, and β_0 is the intercept term. The coefficients β_i ($i = 1, 2, \ldots, k$) represent the linear effects, β_{ii} ($i = 1, 2, \ldots, k$) are the quadratic effects, and β_{ij} ($i = 1, 2, \ldots, k; j = 1, 2, 3, \ldots, k; j \neq i$) are the interaction effects. Finally, ε is the random error term.

TPC and TFC were recorded as response variables. Optimization was conducted by applying a desirability function to find extraction that yielded the maximum TPC and TFC. To validate the model's predictive performance, the extraction process was

Table 2 Matrix of Box–Behnken design with observed responses and prediction error

	Variables			Total phenolic content (g GAE/g sample)		Total flavonoid content (g RE/g sample)	
Run	x_1	x_2	x_3	Actual	Prediction	Actual	Prediction
1	0	0	0	1.70 ± 0.08	1.82	2.41 ± 0.05	2.62
2	0	0	0	1.82 ± 0.04	1.82	2.65 ± 0.13	2.62
3	0	−1	−1	3.04 ± 0.16	3.08	3.92 ± 0.29	3.81
4	−1	0	−1	1.01 ± 0.03	1.01	2.13 ± 0.02	2.17
5	+1	+1	0	1.39 ± 0.02	1.42	2.08 ± 0.08	2.01
6	+1	0	+1	2.30 ± 0.01	2.30	2.51 ± 0.17	2.60
7	−1	0	+1	1.14 ± 0.01	0.98	1.82 ± 0.01	2.46
8	0	0	0	1.94 ± 0.09	1.82	2.79 ± 0.05	2.62
9	−1	−1	0	2.77 ± 0.01	2.73	4.51 ± 0.02	4.59
10	0	+1	−1	0.98 ± 0.07	0.79	1.66 ± 0.04	1.68
11	+1	−1	0	4.44 ± 0.08	4.25	5.52 ± 0.07	5.58
12	+1	0	−1	1.64 ± 0.03	1.80	2.24 ± 0.04	2.29
13	0	+1	+1	0.97 ± 0.01	0.94	1.28 ± 0.04	1.39
14	−1	+1	0	0.64 ± 0.03	0.83	2.79 ± 0.04	2.73
15	0	−1	+1	3.19 ± 0.04	0.94	4.71 ± 0.21	4.69

repeated 3× under optimal conditions, and the experimental data were compared with the 95% prediction interval (PI Low and PI High).

2.5 TPC and TFC determination

The TPC of the extracts was studied applying a UV-Vis spectrophotometer, following the Folin–Ciocalteu colorimetric technique with slight improvement as described by Singleton *et al.*[27] A 0.3 mL of extract was combined with 2.5 mL of tenfold-diluted Folin–Ciocalteu reagent (v/v), and 2.0 mL of sodium carbonate (7.5% w/v) was added. The reaction mixture was incubated for 2 hours at ambient temperature in dark conditions. Absorbance was measured at 760 nm, using gallic acid as the standard for calibration. The findings were expressed as mg of gallic acid equivalent per g of sample (g GAE per sample) which were performed in duplicate.

The TFC was evaluated according to the aluminum chloride colorimetric assay as stated by Blasa *et al.* and Rodríguez-Martínez *et al.*[28,29] A 1 mL of each extract was reacted with 0.3 mL of a sodium nitrite solution (5% w/v) and then with 0.3 mL of an aluminum chloride solution (10% w/v). After 3 minutes incubation at room temperature, the absorbance was observed at 510 nm applying a UV-Vis spectrophotometer. Rutin was applied as the reference compound, and the findings were represented as mg of rutin equivalent per g of sample (g RE per sample). All assays were performed in duplicate.

2.6 Characterization of functional groups with FTIR

The extract functional groups were analyzed applying a Thermo Scientific Nicolet iS10 FTIR spectrometer over the 600–4000 cm^{-1} wavenumber range, with a 8 cm^{-1} resolution. Approximately 1 to 2 mg of the dried sample was introduced to the mixture along with 100 mg KBr (potassium bromide) powder using a hydraulic press and compressed into a clear pellet of KBr. To minimize the spectrum interference, the pellet method of KBr was used to ensure the correct identification of functional groups.

For a liquid sample, such as cacao shell extract, FTIR analysis was carried out using an FTIR spectrometer fitted with an ATR (attenuated total reflectance) accessory. A few drops of the liquid extract were put on the clean surface of the ATR crystal. Measurements were separated by thoroughly drying the ATR crystal using ethanol to avoid sample contamination. The obtained spectra were observed by establishing typical absorption bands of functional groups.

2.7 TGA (thermogravimetric analysis)

TGA was performed to find the thermal stability and the compositional changes of the cacao shell extract residue. The evaluation was conducted out on a PerkinElmer TGA 40000. To avoid oxidative degradation, the sample of approximately 5–10 mg was heated at 10 °C min^{-1} at a linear temperature between 30 and 600 °C in the presence of nitrogen. Subsequently, the thermogram was used to identify the moisture loss, thermal decomposition stage, and the presence of thermally stable components.

2.8 SEM (scanning electron microscopy)

SEM was carried out to observe the surface morphology of the cacao shell extract residue. Before analyzing, the samples were sputter-coated with a carbon (C) thin layer to enhance conductivity. The samples coated were placed on an SEM specimen stub and examined at an 15 kV accelerating voltage using a JEOL JSM-6510LV. The micrographs obtained provided valuable information on structural alterations on the sample surface after extraction.

2.9 Antibacterial activity assay

The samples' antibacterial activity for *E.coli* (ATCC 25922) and *S. aureus* (ATCC 25923) was tested. Initially, the bacterial strain was cultured on the NA (Nutrient Agar) plates and incubated at 35 ± 1 °C for 18–24 hours. The single colonies were transferred to sterile phosphate buffered saline (PBS) and brought up to 1 × 10^8 CFU mL^{-1}, with an optical density of approximately 0.1 at 550 nm or equal to a 0.5 McFarland standard.

The agar well diffusion technique was applied to obtain antibacterial activity. Initially, 1 mL of the standardized bacteria suspension was uniformly distributed on sterile Petri dishes. Mueller-Hinton Agar (MHA) previously equilibrated at 45 ± 1 °C was poured into each Petri dish at a constant volume (20 mL), ensuring uniform distribution for all the plates. After the agar had solidified, 6 mm diameter wells were carefully made applying a sterile cork borer, each filled with 20 μL of the test solution. Positive and negative controls were 10 mg mL^{-1} *trimethoprim* and sterile distilled water, respectively. Subsequently, plates were incubated at 37 °C for exactly 24 hours to achieve equal conditions. Antibacterial activities were obtained by measuring the inhibition zones diameter around the wells. Every assay was conducted 3× to make sure reproducibility.

2.10 Statistical analyses

The TPC and TFC extraction optimization was performed applying Design-Expert software version 13 (Stat-Ease Inc., Minneapolis, MN, USA) through RSM-BBD. ANOVA (Analysis of variance) at the $p < 0.05$ level of significance was conducted to assess the impact of the individual factors and their interactions with each other. The model adequacy was checked by making comparation of experimental results with the results predicted in the 95% prediction interval (PI Low-PI High).

Antibacterial activity, inhibition zone diameter on *E. coli* and *S. aureus*, TPC, and TFC values were statistically analyzed applying Statgraphics Centurion version 18 (Statgraphics Technologies, The Plains, VA, USA). Data were obtained as mean ± SD (standard deviation) of duplicate measurements. In determining significant differences among treatments ($p < 0.05$), one-way ANOVA followed by Tukey's post hoc test was conducted. Different superscript letters were used to denote statistically significant differences.

3 Result and discussion

3.1 Effect of mass transfer extraction on the flavonoid content of cacao shell extracts

Understanding mass transfer during solid–liquid extraction is essential for maximizing the bioactive compounds recovery.[30] Several parameters influence the mass transfer of compounds during SAE-DES. The solvent composition, solid-to-solvent ratio, temperature, and extraction period affect the extraction rate and yield.[31] In this cacao shell extraction, mass transfer is measured more specifically by TFC, which reflects the transfer of flavonoid compounds, rather than TPC. This is done because cacao shells contain high levels of flavonoids, making them more representative and allowing for a more accurate evaluation of mass transfer efficiency. The mass transfer efficiency was determined using TFC as a marker. This method provided critical insight into the impact of extraction parameters on bioactive yield to guide the development of sustainable and scalable extraction processes.[32]

This study tested three parameters, namely temperature, solid to solvent ratio, and concentration of DES, with samples collected at specific time intervals. The extraction parameters showed significant impacts on the mass transfer coefficient ($k_c a$) and equilibrium constant (H_s) in the extraction of TFC from cacao shell, as shown in Table 3. Theoretically, the temperature rise would increase the mass transfer. However, the opposite was observed in this analysis, as the extract indicated the highest concentration of TFC at 80 °C with a mass transfer coefficient ($k_c a$) of 8.88×10^3 min^{-1} and is smaller than the other two data points. At the same time, the extract showed a high equilibrium constant of 9.33×10^3 g solid per cm^3, which increased mass transfer's driving force and produced higher TFC. The huge yield increase of TFC at 80 °C could be attributed to enhanced solute diffusion and plant matrix expansion, increasing the surface area of the solvent penetration.[33] This provides higher yields of bioactive extract compared to those obtained at lower temperatures.

Table 3 Effect of extraction variables on mass transfer and equilibrium behavior

	Temperature (°C)		
Parameters	40	60	80
$k_c a$ (min^{-1})	14.80×10^{-3}	12.53×10^{-3}	8.88×10^{-3}
H_s (g solid per cm^3)	1.59×10^{-3}	3.98×10^{-3}	9.33×10^{-3}
R^2	0.79	0.88	0.95
Error (%)	0.10	0.29	0.64
	Ratio solid : solvent		
Parameters	1 : 10	1 : 25	1 : 40
$k_c a$ (min^{-1})	8.73×10^{-3}	9.89×10^{-3}	11.16×10^{-3}
H_s (g solid per cm^3)	41.91×10^{-3}	10.79×10^{-3}	0.56×10^{-3}
R^2	0.95	0.91	0.89
Error (%)	9.19	1.35	0.24
	DES concentration (%)		
Parameters	50	75	100
$k_c a$ (min^{-1})	12.93×10^{-3}	12.08×10^{-3}	8.88×10^{-3}
H_s (g solid per cm^3)	13.89×10^{-3}	10.36×10^{-3}	9.33×10^{-3}
R^2	0.98	0.97	0.95
Error (%)	0.54	0.42	0.64

According to the data-fitting shown in Table 3, the solid-to-solvent ratio influences both mass transfer and the equilibrium constant. At a lower ratio, solvent availability is abundant, allowing an increase in the extraction rate. As shown in Table 3, a solid-to-solvent ratio of 1 : 40 produced the highest mass transfer rate constant (11.16×10^{-3} min^{-1}) among the data. However, at a lower ratio, the resulting equilibrium constant (H_s) is smaller than the other data. This is due to the low solid content in the system, which limits the solvent's availability around the solid and results in a lower TFC yield.

In addition to temperature and the solid-to-liquid ratio, the DES concentration also affects the values of $k_c a$ and H_s. An increase in DES concentration causes an increase in viscosity, which can hinder diffusion and solvent penetration.[34] Consequently, the mass transfer rate decreases, as the calculated $k_c a$ value (8.88×10^{-3} min^{-1}) at a concentration of 100% is lower than the other data. In addition to causing decreased viscosity, a reduction in concentration could lead to high conductivity, which enhances the rate of mass transfer.[35,36] Among the tested DES concentration variations, 50% DES showed an optimal balance of physicochemical properties, with high $k_c a$ (12.93×10^{-3} min^{-1}) and H_s (13.89×10^{-3} g solids per cm^3) values. These results suggest that partial hydration of DES is necessary to achieve an effective solvent system that maintains adequate solubility for the extraction of flavonoid compounds.[37]

Even though Table 3 provides a quantitative overview of mass transfer parameters, a deeper understanding of the extraction dynamics can be gained from the mass transfer profiles shown in Fig. 1. Fig. 1(a) shows the impact of temperature and extraction time on TFC. As shown in the graph, TFC tends to increase with rising temperatures. The TFC values under equilibrium conditions at 80 °C, 60 °C, and 40 °C were 9.33×10^{-3} g solid per cm^3, 3.98×10^{-3} g solid per cm^3, and 1.59×10^{-3} g solid per cm^3, respectively. Based on this finding, the increase in temperature results in a higher equilibrium constant, suggesting that the process is endothermic. A similar trend has also been reported previously on the polyphenols extraction from cacao shell and other plants, where the yield of bioactive extracts increases with increasing temperature and with the use of the sonication method for extraction[38,39] Moreover, the impacts of the solid-to-solvent ratio and extraction duration on TFC are illustrated in Fig. 1(b). The highest TFC was obtained at a ratio of 1 : 10 and declined with further reductions in the ratio. The lowest TFC value under equilibrium conditions was obtained at a 1 : 40 ratio, with a value of 0.56×10^{-3} g solid per cm^3.

The DES concentration parameter at various times also affects the TFC results, as shown in Fig. 1(c). Based on the graph, an increase in DES concentration in a decrease in TFC. The optimum condition occurs at a DES concentration of 50% with an equilibrium yield of 13.89×10^{-3} g RE per cm^3. This

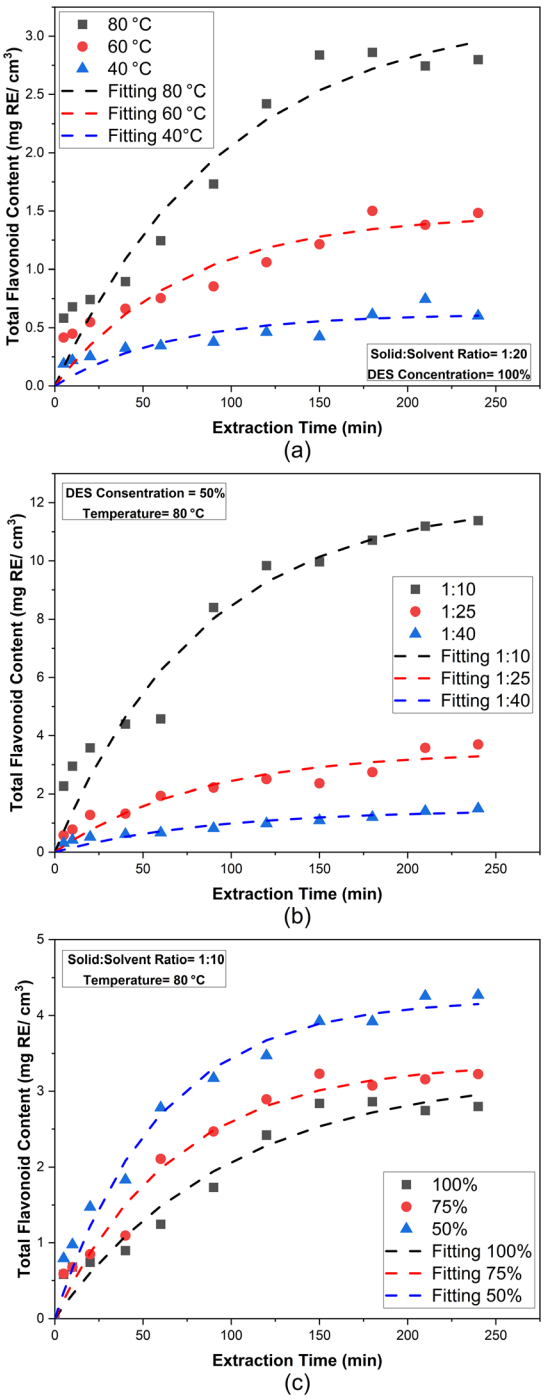

Fig. 1 TPC in SAE-DES under varying conditions: (a) extraction temperature, (b) solid-to-solvent ratio, and (c) DES concentration. Values represent mean ± S.D. ($n = 2$).

value is higher than the yields at 75% and 100% solvent concentrations, with TFC yields of 10.36 × 10^{-3} and 9.33 × 10^{-3} g RE per cm^3, respectively. This decrease is influenced by the solvent's physicochemical characteristics, with higher DES concentration leading to increased viscosity. Under these conditions, solvent penetration and mass transfer within the cacao shell matrix can be hindered.[40]

3.2 Optimization of extraction conditions

Following the investigation of parameter effects on the integration of SAE-DES extraction with respect to mass transfer and equilibrium constant, an optimization analysis was performed. Multivariate analysis revealed that the quadratic model exhibited a statistically significant p-value ($p < 0.05$) for TPC and TFC, confirming its suitability for predicting the response (Table S1). From the ANOVA analysis results (Table 4), both models exhibited high F-values, specifically 34.97 for TPC and 66.83 for TFC. This indicates that the models used are statistically significant. This is reinforced by the p-values for each model being < 0.05, which confirms that the selected independent variables and their interactions generally affect the response. Additionally, the lack-of-fit analysis results, which indicate the error variable, yield p-values of 0.178 for TPC and 0.588 for TFC. This shows the lack of fit is not significant, thereby enhancing model accuracy. In addition to traditional statistical metrics, such as R^2 and p-values, the model's predictive power was also confirmed by the strong relationship between experimental and TPC and TFC predicted values in Fig. S1. The results showed that data points were clustered around the line of identity, indicating low prediction error as well as the robustness and usefulness of the model for process optimization.

Statistical optimization of the operating conditions in SAE using DES for the recovery of TPC and TFC was performed with the RSM. Several parameters were optimized, including temperature, solid and solvent ratio, and DES concentration. The effect of each parameter was further examined using main effect graphs, as presented in Fig. S2. These graphs show the variations between independent (temperature, solid/solvent ratio, and DES concentration) and dependent variables (TPC and TFC). Additionally, the importance and directionality of individual factors and factor interactions on TPC and TFC, as determined by multivariate analysis (standardized Pareto charts, Fig. S3) is shown. Based on the results, significant interaction effects further confirm the complex interdependency of the extraction variables.

As shown in Fig. 2, three-dimensional graphs were provided to visually identify the interaction of each parameter on the responses obtained. A regression model was constructed using coded variables, which contained linear, interaction, and quadratic terms to comprehensively describe the multifactorial correlation between process parameters and response variables. These models explained the temperature impacts, solvent-to-sample ratio, and DES concentration on yields of TPC and TFC. The addition of interaction and curvature terms increased the model's capacity to accurately represent real experimental behavior, thereby improving the predictive power for process optimization. The final regression equations in terms of code variables are shown below.

$$\begin{aligned}\mathrm{TPC} = {} & 1.64 + 0.0372x_1 - 0.1403x_2 + 0.0360x_3 - 0.000041{x_1}^2 \\ & + 0.002255{x_2}^2 - 0.000448{x_3}^2 - 0.000769x_1x_2 \\ & + 0.000266x_1x_3 - 0.000103\ x_2x_3 \end{aligned} \quad (12)$$

Table 4 ANOVA and fits statistics of the response variables[a]

	Total phenolic content (RGE)				Total flavonoid content (RE)			
Source	SS	MS	*F*-Value	*p*-Value	SS	MS	*F*-Value	*p*-Value
Model	15.13	1.68	34.97	0.001	20.67	2.30	66.83	0.000
Linear								
x_1	2.22	2.22	46.21	0.001	0.00	0.00	0.02	0.906
x_2	11.18	11.18	232.61	0.000	14.72	14.72	428.28	0.000
x_3	0.10	0.10	2.18	0.200	0.04	0.04	1.24	0.316
Quadratic								
${x_1}^2$	0.00	0.00	0.02	0.891	0.18	0.18	5.38	0.068
${x_2}^2$	0.95	0.95	19.77	0.007	2.89	2.89	84.03	0.000
${x_3}^2$	0.29	0.29	6.02	0.058	1.37	1.37	40.00	0.001
Interaction								
x_1	0.21	0.21	4.42	0.089	0.73	0.73	21.25	0.006
x_2	0.07	0.07	1.47	0.279	0.08	0.08	2.41	0.181
x_3	0.01	0.00	0.12	0.740	0.34	0.34	10.02	0.025
Fit statistic								
Lack of fit	0.21	0.07	4.78	0.178	0.09	0.03	0.83	0.588
R^2	0.9844				0.9918			
Adj. R^2	0.9562				0.9769			

[a] SS: sum of squares; MS: mean square.

$$\mathrm{TFC} = 2.81 - 0.0176x_1 - 0.1624x_2 + 0.1374x_3 + 0.000560{x_1}^2 + 0.003931{x_2}^2 - 0.000976{x_3}^2 - 0.001424x_1x_2 - 0.000288x_1x_3 - 0.000782x_2x_3 \quad (13)$$

x_1, x_2, and x_3 represent the SAE-DES factors (temperature (x_1), ratio solid: solvent (x_2), and DES concentration (x_3)).

The response surface plots obtained from this study were optimal at the corners of the design space instead of the center point. According to the graph in Fig. 2(a), the phenolic yield was found to be continuously increased with rising temperature and decreasing the solid-to-solvent ratio. This is a mixed impact of enhanced mass transfer as well as delignification reactions during sonication and DES treatment. At high temperature, molecular diffusion coefficient increases, thereby reducing mass transfer resistance through plant cell walls. Simultaneously, DES, composed of choline chloride and lactic acid, plays a role in disrupting the lignin structure through hydrogen bonding and mild acid hydrolysis, leading to partial delignification.[41] This can enhance porosity and weaken the cellulose-lignin matrix, thus increasing solvent access to intracellular phenolic compounds. The findings indicate a significant difference compared with a previous study that used the RSM optimization method with sonication and ethanol as the solvent.[42] In that study, the maximum TPC obtained was only 0.26 g GAE per sample, whereas in this study it reached 4.44 g GAE per sample. This considerable difference is thought to be due to ethanol's limited ability to disrupt the lignocellulosic matrix, particularly lignin, in cacao shell, leading to suboptimal release of phenolic compounds. In addition, at a low solvent-to-solute ratio, solvent dissolution and transport are more efficient. This condition can reduce the concentration gradient and prevent local saturation.[43] To strengthen the results of this analysis, TGA (thermogravimetric analysis) and SEM (scanning electron microscopy) were carried out.

Optimization was carried out to maximize TPC and TFC yields while still considering feasibility and operational efficiency. In this optimization, three parameters were tested: temperature at approximately 40 °C and 80 °C, solid-to-solvent ratio of 1 : 10 to 1 : 40, and DES concentration of 25–75%. Optimization conducted applying the desirability function approach with two responses, TPC and TFC, which were assigned to the highest importance level (+++++). The optimum conditions were obtained at 80 °C, a solid-to-solvent ratio of 1 : 10, and a DES concentration of 62.65%. Under these conditions, the model predicted an overall desirability value of 0.982, showing a good balance between the two target responses. A desirability value close to 1 signifies a high level of prediction accuracy. In this study, the slightly lower desirability value reflects a compromise between optimal conditions for maximizing TPC and TFC, in which higher DES concentrations tend to enhance TPC extraction. In contrast, slightly lower concentrations are more suitable for maximizing TFC.

To validate the optimization results, calculations were performed under the optimum conditions three times. The comparison between experimental results and predictions is presented in Table 5. The average TPC and TFC values were 4.94 ± 0.10 g GAE per g sample and 5.97 ± 0.09 g RE per g sample, respectively. These values are very close to the predicted model values (4.32 and 5.46, respectively) and fall within the 95% PI (prediction interval), thus confirming the reliability and accuracy of the obtained regression model.

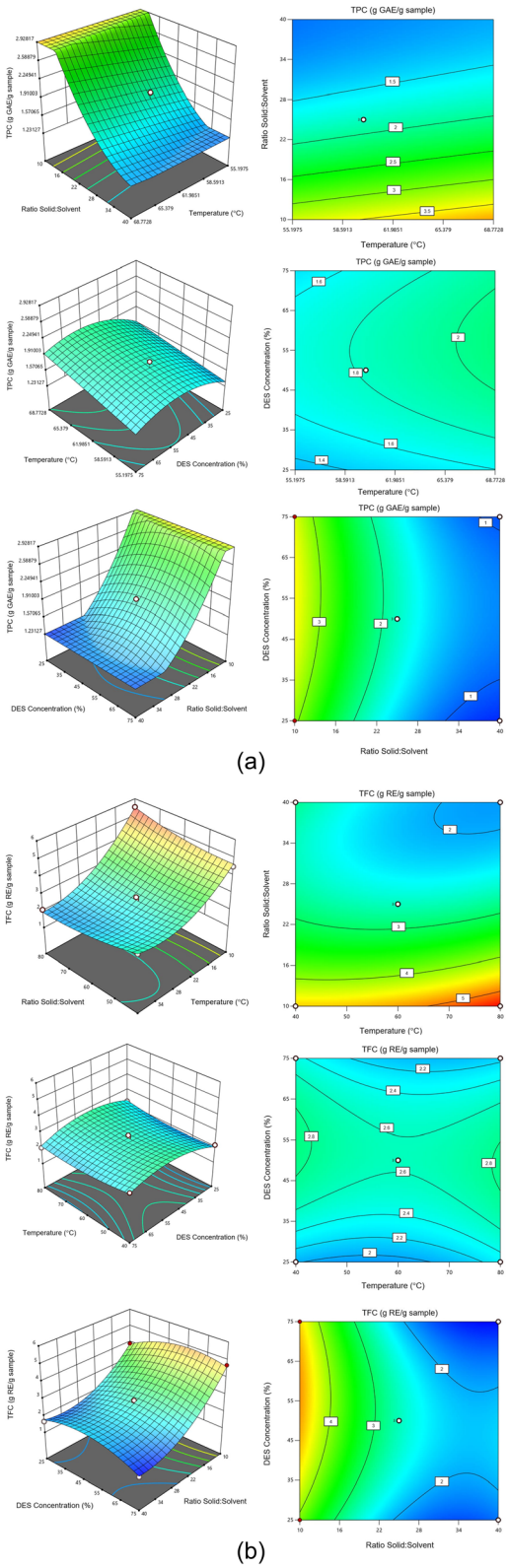

Fig. 2 Response surface 3D depicting the impacts of SAE-DES factors on TPC (a) and TFC (b) levels in the extract of cacao shells.

3.3 FTIR analysis and characterization of cacao shell extracts and residues

FTIR spectroscopy was applied to analyze structural changes and functional group evolution in cacao shell residues following SAE–DES extraction under varying temperatures and extraction times (Fig. 3). This analysis provides insight into the extraction selectivity and interaction mechanisms of the DES system toward phenolic compounds, flavonoids, polysaccharides, and lignin-derived structures. In the high-wavenumber region (3600–3200 cm^{-1}), all samples exhibited a broad absorption band corresponding to –OH and –NH stretching vibrations associated with hydroxyl- and amine-containing bioactive compounds, including phenolics, flavonoids, and water-soluble polysaccharides.[44–46] A decrease in absorption intensity was observed at higher temperatures and longer extraction duration. This indicates that, hydrophilic components are significantly lost. A progressive decrease in band intensity, in the peak around 3272–3300 cm^{-1}, was observed at higher temperatures and longer extraction times, indicating depletion of hydrophilic components and reduced hydroxyl content because of strong hydrogen-bonding interactions with DES components. The results are consistent with Wang *et al.*,[47] which showed that a similar spectral trend is observed in plant matrices during extraction.

Meanwhile, –CH stretching vibrations at 2920–2850 cm^{-1} were observed in the FTIR results of all samples. This indicates the presence of aliphatic chains, methyl groups, and methylene groups, which are commonly found in lignin, lipids, or waxy components. This suggests a moderate decrease in peak intensity with increasing extraction temperature and duration. The weakening of –CH groups, especially at 360 minutes, indicates partial solubility or disruption of aliphatic groups due to prolonged sonication. Additionally, the spectral feature in the 1740–1600 cm^{-1} range indicates the absorption of carbonyl and aromatic compounds.[46] The observed C=O stretching band at 1738–1732 cm^{-1} is correlated with esterified phenolic compounds or lignin derivatives. The data show a decrease in intensity and a slight shift toward lower wavenumbers after extraction, especially at 80 °C and longer extraction times. Similarly, the aromatic C=C stretching band (1647–1613 cm^{-1}) shows a slight shift in position and a decrease in intensity. This indicates successful extraction of the flavonoid backbone and aromatic-rich compounds.[48] However, some of these bands are still detected even after 360 minutes of extraction. This suggests the presence of lignin structures that resist complete dissolution, as explained by Giummarella and Lawoko (2017).[49]

In the fingerprint region (1400–1000 cm^{-1}), pronounced reductions in C–O and C–O–C stretching bands characteristic of polysaccharides and phenolic ethers were observed, reflecting the removal of soluble carbohydrates and ether-linked phenolics.[50,51] The emergence of new bands in post-extraction residues and attenuation of signals below 1000 cm^{-1} further indicate structural rearrangement and degradation of the cacao shell matrix. This is likely due to structural disintegration and progressive damage to the cacao shell matrix. In addition to the spectrum of the extraction residue, Fig. 3 also shows reference spectra of pure lignin and cellulose. All residue spectrum shows

Table 5 Verification of predicted and experimental values under optimal conditions

Analysis	Predicted mean	Predicted median	Std Dev	*n*	95% PI low	Data mean	95% PI high
TPC	4.32	4.32	0.22	3	3.71	4.94	4.94
TFC	5.46	5.46	0.19	3	4.94	5.97	5.98

a higher similarity to cellulose than to lignin. This indicates that during the extraction process, some lignin compounds and phenolic compounds tend to dissolve and migrate from the solid phase into the solvent, leaving behind a solid fraction richer in cellulose. In general, these FTIR results confirm that increasing the extraction temperature and time plays a role in enhancing the release of bioactive compounds, particularly those derived from phenolic and lignin components, while the more resistant lignocellulosic structures, especially cellulose, remain in the solid residue.

The DES spectrum from Fig. 4 shows characteristic absorptions of the hydrogen bond-contributing component (donor), lactic acid, and the hydrogen bond-accepting component (acceptor), choline chloride, with broadening and merging of the –OH and –NH stretching bands (~3296 cm^{-1}). This indicates strong hydrogen bonding interactions. Upon the addition of the cacao shell extract, the –OH band becomes more intense. This condition indicates the presence of phytoconstituents rich in hydroxyl groups that have been successfully extracted from the matrix. Several previous studies have also identified the flavonoid phytoconstituent quercetin in cacao shell.[52,53] The quercetin structure contains a significant number of hydroxyl groups at positions C-3, C-5, C-7, C-3′, and C-4′, which correlates directly with the increase in the –OH peak in the extract spectrum.[54] In addition to the hydroxyl group, new peaks at 1731 cm^{-1} and 1646 cm^{-1} in the extract–DES mixture are related to C=O stretching and aromatic C=C vibrations, indicating the presence of carbonyl- and aromatic-rich compounds, which is consistent with the vibrational modes reported for quercetin. Previous studies conducted using Raman spectroscopy support the presence of several bioactive compounds, one of which is a flavonoid such as quercetin.[45] Although these spectral characteristics are very similar to those of quercetin, the overlap of vibrational bands in the FTIR spectrum suggests the possible presence of other structurally related polyphenolic or aromatic compounds, such as other flavonoids, in the extract.

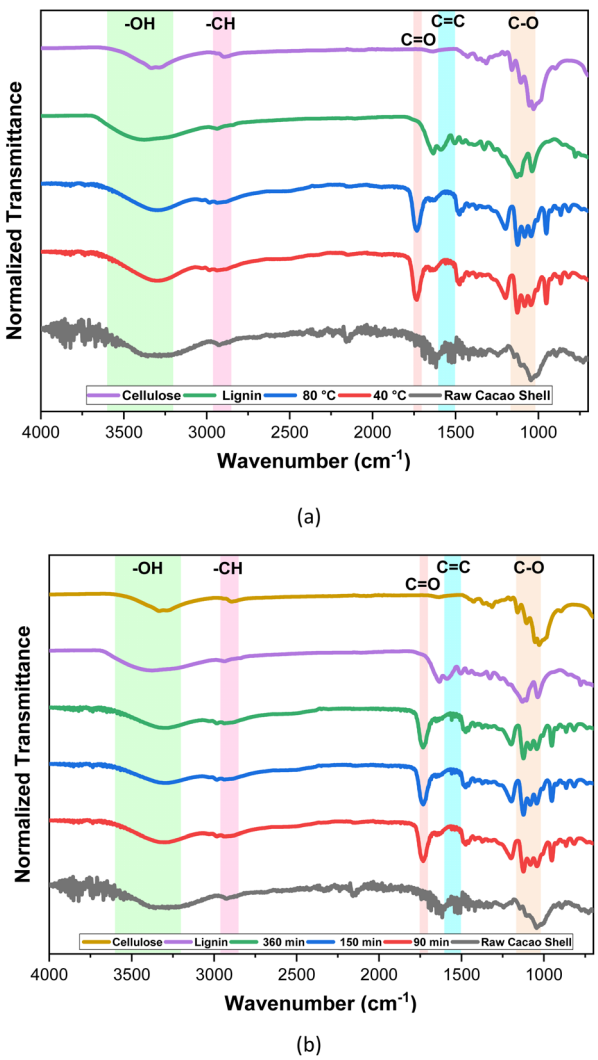

Fig. 3 Fourier transform infrared (FTIR) spectra of cacao shell residues under varying extraction temperature (a) and time (b).

3.4 Thermogravimetric analysis of cacao shell

In assessing the thermal stability and compositional changes in cacao shells before and after solvent-assisted eutectic sonication (SAE-DES) extraction, TGA was performed. A total of two

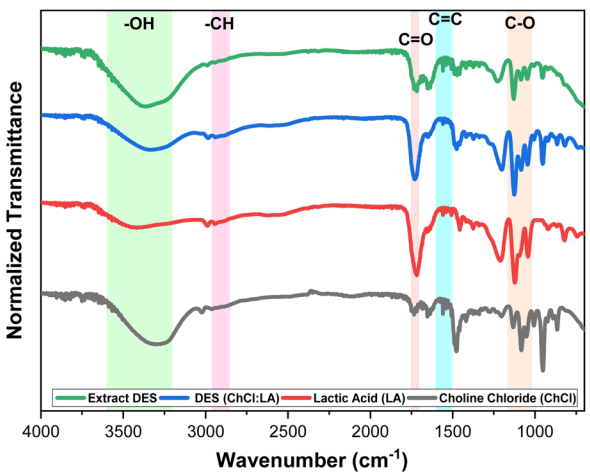

Fig. 4 FTIR spectra of individual components (choline chloride and lactic acid), the synthesized deep eutectic solvent (DES; ChCl : LA), and the cacao shell extract obtained using the DES.

samples were analyzed at 40 and 80 °C, with the results shown in Fig. 5. Based on the TGA curves shown, the residual biomass in each sample showed a three-stage thermal decomposition pattern. In the first stage, up to 130 °C, there was a slight loss in mass for all samples related to the evaporation of physically adsorbed and bound water. This stage is related to the free water desorption and weakly bound intrafibrillar water molecules, as reported earlier in lignocellulosic biomass.[55]

In the second stage of degradation (200 to 350 °C), large amounts of mass loss are associated with the depolymerization and volatilization of hemicellulose (220–315 °C) and cellulose (300–400 °C).[56] The untreated cacao shells had a wider shoulder of degradation, implying a more disorganized structure of the structure. Meanwhile, the SAE – DES desiccated residues, particularly the extracts at 80 °C, had a thinner and tighter degradation profile, suggesting simplification of the structure. The lower maximum decomposition temperature of the 80 °C residue indicates lower thermal stability due to increased removal of thermally stable components, including lignin and condensed phenolics.[57]

At the final degradation stage at temperatures above 350 °C, thermal degradation is related to the slow carbonization process of lignin and other resistant aromatic structures. Lignin has a large range of degradation (150–900 °C) due to its complex and cross-linked structure. In Fig. 5, the residual mass of SAE-DES 80 °C residue sample is less compared to others. This indicates that the sample had more delignification than the SAE-DES 40 °C residue and the untreated sample. This pattern positively correlates with the increased TPC recorded in the corresponding extracts, indicating the efficient dissolution of lignin-derived phenolic groups at high temperatures of extraction. Overall, the results of TGA analysis show the structural changes in cacao shell biomass due to SAE-DES extraction. This thermal behavior shows that high extraction temperatures favor the release of phenolic and lignin constituents, thereby leaving residues with greater susceptibility to thermal degradation.

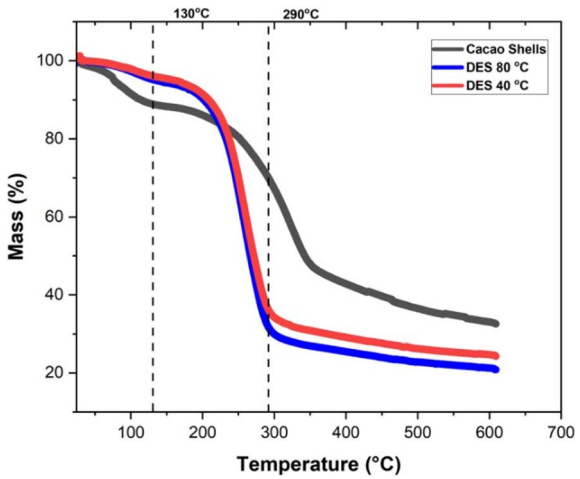

Fig. 5 Thermogravimetric analysis (TGA) curves of cacao shells and DES residues obtained from extractions at 40 °C and 80 °C.

3.5 SEM characterization of cacao shell before and after extraction

Cacao shell samples after experiencing the integrated SAE-DES were examined on SEM to observe their structure. This analysis was performed to investigate the morphological variations of cacao shells for various temperatures and extraction times. Fig. 6 shows the SEM results of samples extracted at (a) 40 °C and 80 °C and (b) 90 and 360 minutes. Unextracted cacao shell biomass shows a smooth, dense, and continuous surface with block-like features, reflecting intact lignocellulosic cell walls made up of lignin, hemicellulose, and pectin. The components of these cell walls bind the matrix of the fiber, which hinders the release of the intracellular bioactive compounds, like phenolic compounds.[58,59]

In Fig. 6(a), that after the extraction process at high temperature (80 °C), a significant morphological difference is evident. Larger pores and cavities are observed in the cell wall structure compared to extraction at 40 °C, which reveals relatively minor cavities. This increase in porosity is attributed to delignification during the DES process at high temperatures. This result is confirmed by thermogravimetric analysis (TGA), which shows significant lignin degradation.[60] The

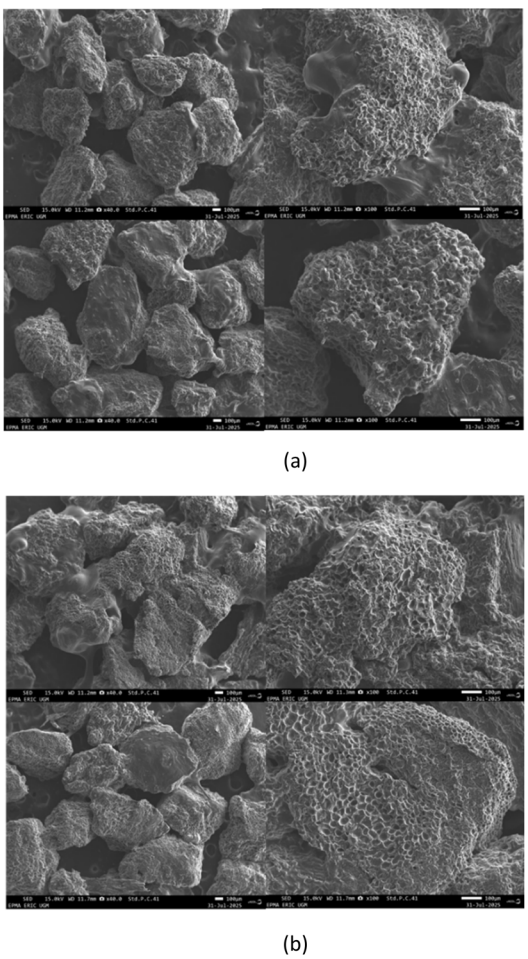

Fig. 6 SEM analysis of structural alterations in extraction residues under the influence of (a) temperature (40 and 80 °C) and (b) extraction duration (90 and 360 min).

Table 6 Effect of TPC and TFC on antibacterial testing results for *E. coli*[a]

Code	Temperature (°C)	Extraction time (min)	TPC (g GAE per g sample)	TFC (g RE per g sample)	Inhibition zone (mm)
DES-1	80	90	0.24 ± 0.00	0.07 ± 0.01	27.67 ± 2.08[b]
DES-2	80	150	0.49 ± 0.00	0.16 ± 0.00	30.33 ± 1.04 [ab]
DES-3	80	180	0.65 ± 0.00	0.11 ± 0.00	33.33 ± 0.21 [ab]
DES-4	80	360	1.35 ± 0.01	0.15 ± 0.02	27.33 ± 0.58[b]
DES (ChCl : LA)					24.33 ± 2.03[a]
Positive control					39.67 ± 3.95[b]

[a] Average ± SD; $n = 3$; GAE = gallic acid equivalent; RE = rutin equivalent.

delignification process causes the breakage of lignin-carbohydrate complexes, thereby weakening the cell wall structure and allowing the solvent to penetrate.[61] As a result, larger pores are formed, which enhance mass transfer by increasing solvent accessibility and diffusion pathways. In this case, the phenolic compounds are facilitated in their mass transfer from the solid matrix into the solvent. SEM results also indicate that the delignification process continues to occur at the maximum tested temperature. This finding aligns with TGA results, which show that lignin degradation continues at temperatures above 80 °C. The continuous degradation is attributed to high temperature, which will increase the delignification process and contact between the solvent and the matrix. This interaction was projected to improve the extraction efficiency more than was recorded in this study.

The combined use of DES and cavitation caused by SAE is significant in the destabilization of cell walls. Specifically, sonication causes microbubbles due to speedy shifts in pressure between compression and expansion phases. These bubbles burst release mechanical shear forces with the ability to rupture plant tissues. The process is referred to as cavitation, which enables the operation of DES in infiltrating plant tissues and solubilizing lignin. The dissolution of lignin takes place depending on the dipole–dipole interaction and the hydrogen bonding.[62] The two effects are combined to dissolve bioactive compounds of cell wall components and lignin.

The residues of the cacao shells were extracted after 90 and 360 minutes, with the difference shown in Fig. 6(b). The extraction process using the longer SAE-DES method showed SEM results, where fiber breakage and tissue collapse were observed. These modifications indicated gradual disintegration of cell walls, which correlated with the process of delignification. This promotes an increased mass transfer and greater release of intracellular compounds. This finding is supported by kinetic and diffusion analysis in related studies, which reported higher Biot numbers and effective diffusivity coefficients in DES-based systems. Research conducted by Lee *et al.*[63] demonstrated an accelerated mass transfer process of phenolic compounds from biomass to solvent, attributed to the turbulence induced by sonication and the strong solubilizing power of DES.

3.6 Antibacterial analysis of cacao shell extract

The extract of cacao shells obtained using SAE-DES was tested for its antibacterial activity. The evaluation was conducted against Gram-negative bacteria (*E. coli* ATCC 25,922) and Gram-positive bacteria (*S. aureus*) applying the agar well diffusion method. Testing against *E. coli* was performed on extracts produced at 80 °C with extraction times of 90, 150, 180, and 360 minutes, as listed in Table 6. To compare the effects of the extract, tests were also conducted on the single DES solvent and the positive control (*Trimethoprim*). For all durations tested, the inhibition zone against *E. coli* was generally quite large. This indicates a strong bactericidal potential.

The highest antibacterial activity was observed in the extract, with an inhibition zone diameter of 33.33 ± 0.21 mm, which was statistically equivalent to that of the positive control (39.67 ± 3.95 mm, $p > 0.05$). This result was obtained from a sample with an extraction time of 180 minutes. The potent inhibition of *E. coli* by this cacao shell extract can be attributed to multiple synergistic antimicrobial mechanisms produced by the phenolic compounds, flavonoids, and organic acids present in the extract.

There are four possibilities in this process. First, these bioactive compounds inhibit bacteria's efflux pumps, thereby averting the release of toxic substances and enhancing intracellular amassing of antibacterial agents. Second, the flavonoids also interact with bacterial ribosomes, restraining the production of proteins and interfering with important metabolic processes. Third, polyphenols prevent the activity of DNA gyrase, entangling the DNA and interfering with the replication process. Fourth, amphiphilic phenolic compounds and organic acids have the capacity to destabilize the bacteria cell membrane, causing leakage of the cytoplasm and loss of cell viability.[64,65]

According to the data presented in Table 6, the inhibition zone diameter dropped in the sample with the extraction time of 360 minutes, despite higher TPC. The reduction is due to thermal degradation of thermostable antibacterial agents, such as quercetin, catechins, and other flavonoids, or structural

Table 7 Antibacterial capacity of the optimum cacao shell extract

Bacteria	Inhibition zone (mm) *S. aureus*
Trimethoprim (positive control)	22.67 ± 0.29[b]
Optimum extract DES	28.83 ± 0.76[a]
DES (ChCl : LA)	21.17 ± 5.75[b]
Distilled water (negative control)	0.00 ± 0.00[c]

changes that decrease bioavailability and membrane permeability.[66]

DES solvent (ChCl : LA) alone also showed relatively high antibacterial activity (24.33 ± 2.03 mm). This finding supports previous studies stating that NaDES (natural deep eutectic solvents) containing organic acids have intrinsic antimicrobial properties due to their low pH (1.28 ± 0.25) and their ability to denature proteins in microbial cell membranes.[67] Another study reported an inhibition zone of 5.26 ± 0.71 mm for extracts obtained from conventional ethanol extraction of cacao shell against *E. coli*.[65] Interestingly, the inhibition zone produced by extraction using the SAE-DES method can generate a larger inhibition zone. This confirms the synergistic effect between choline chloride and lactic acid when combined with ultrasonication, thereby significantly increasing the yield of phenolic compounds.

The antibacterial properties of the extract were also tested on *S. aureus*, as shown in Table 7. Analysis of the optimal cacao shell extract resulted in 28.83 ± 0.76 mm inhibition zone. This value is larger than that of *trimethoprim* (positive control), which has an inhibition zone of 22.67 ± 0.29 mm ($p < 0.05$). This confirms that cacao shell extract obtained using SAE-DES exhibits strong bactericidal efficacy. According to a study reported by Álvarez-Martínez *et al.*,[68] plant extracts rich in polyphenols show greater inhibitory activity against Gram-positive bacteria. This occurs because the thick but porous peptidoglycan layer allows the penetration of small antimicrobial molecules, unlike the outer lipopolysaccharide layer in Gram-negative bacteria, which acts as a barrier.

However, in this study, the cacao shell extract showed higher activity against *E. coli* than against *S. aureus*, contrary to previous studies. This unusual result is because of the unique phenolic and flavonoid profile of cacao shell. The content of low-molecular-weight hydrophilic phenolic compounds and abundant organic acids is suspected to penetrate the porin channels of Gram-negative bacteria, thereby disrupting the integrity of their cytoplasmic membrane.[69] Additionally, extraction using the DES method enables the increased recovery of small and polar bioactive compounds by modifying their ionization state. This can increase the permeability of the compound to pass through the outer membrane of Gram-negative bacteria. The synergistic interaction between the acidic DES environment (pH 1.28) and polyphenol compounds can also further weaken the *E. coli* cell wall through a combination of acid stress and oxidative damage, which explains the remarkable inhibitory activity observed.[70]

4 Conclusions

This study demonstrated the potential of DES (ChCl : LA) in extracting bioactive compounds from cacao shell waste. Temperature, solids-to-solvent ratio, and DES concentration can significantly impact the concentration of bioactive compounds extracted, as determined by TPC and TFC analyses. The process registered mass transfer coefficient ($k_c a$) and equilibrium constant (H_s) ranges of 8.73 × 10^{-3} to 14.80 × 10^{-3} min^{-1} and 0.56 × 10^{-3} to 41.91 × 10^{-3} g solid per cm^3, respectively. The results of RSM optimization with BBD indicated that the optimal operating conditions were 80 °C, a solids-to-solvent ratio of 1 : 10, and a DES concentration of 62.65%, yielding extracts with the highest content of bioactive compounds. FTIR spectral analysis confirmed the existence of bioactive compounds, which showed potential as antibacterial agents through *E. coli*. and *S. aureus* growth inhibition.

Conflicts of interest

The authors declare that they have no known competing financial interests or personal relationships that could have appeared to influence the work reported in this paper.

Data availability

The data supporting the findings of this study are available within the article and its supplementary information (SI). Additional data related to this work are available from the corresponding author upon reasonable request. Supplementary information: statistical validation model fitness, predictive performance of the regression model for TPC and TFC responses, effect of individual extraction parameters (extraction time, temperature, and DES concentration) on total phenolic content (TPC) and total flavonoid content (TFC), and also the main, interaction, and quadratic effects of the UAE variables on TPC levels and TFC levels in the extracts. See DOI: https://doi.org/10.1039/d6ra01724j.

Acknowledgements

The authors are grateful to the Indonesian Endowment Fund for Education (LPDP) through the Indonesia-NTU Singapore Institute of Research for Sustainability and Innovation (INSPIRASI) (Number: 6636/E3/KL.02.02/2023) for the financial support.

References

1 P. R. Yaashikaa, P. Senthil Kumar and S. Varjani, Valorization of agro-industrial wastes for biorefinery process and circular bioeconomy: A critical review, *Bioresour. Technol.*, 2022, **343**, 126126, DOI: 10.1016/j.biortech.2021.126126.

2 S. N. Izzah, E. Brugman, T. T. Baladraf and F. Rachmadita, An overview of cocoa nibs shell waste potential to achieve sustainable agriculture, *IOP Conf. Ser. Earth Environ. Sci.*, 2023, **1230**, 012028, DOI: 10.1088/1755-1315/1230/1/012028.

3 O. Rojo-Poveda, L. Barbosa-Pereira, G. Zeppa and C. Stévigny, Cocoa bean shell—a by-product with nutritional properties and biofunctional potential, *Nutrients*, 2020, **12**, 1123, DOI: 10.3390/nu12041123.

4 M. Renna, C. Lussiana, L. Colonna, V. M. Malfatto, A. Mimosi and P. Cornale, Inclusion of Cocoa Bean Shell in the Diet of Dairy Goats: Effects on Milk Production Performance and Milk Fatty Acid Profile, *Front Vet Sci*, 2022, **9**, 848452, DOI: 10.3389/fvets.2022.848452.

5 N. V. de R. Mudenuti, A. C. de Camargo, S. M. de Alencar, R. Danielski, F. Shahidi, T. B. Madeira, *et al.*, Phenolics and alkaloids of raw cocoa nibs and husk: The role of soluble and insoluble-bound antioxidants, *Food Biosci*, 2021, **42**, 101085, DOI: 10.1016/j.fbio.2021.101085.
6 M. Wijaya and M. Wiharto, Synthesis and characterization of bioactive compound from Cocoa fruit shell by pyrolysis process, *J. Phys. Conf. Ser.*, 2020, **1567**, 022025, DOI: 10.1088/1742-6596/1567/2/022025.
7 S. H. Hassanpour and A. Doroudi, Review of the antioxidant potential of flavonoids as a subgroup of polyphenols and partial substitute for synthetic antioxidants, *Avicenna J Phytomed*, 2023, **13**, 354–376, DOI: 10.22038/AJP.2023.21774.
8 I. F. Rusina, T. L. Veprintsev and R. F. Vasil'ev, Antioxidant Activity of Diatomic Phenols, *Russ. J. Phys. Chem. B*, 2022, **16**, 50–57, DOI: 10.1134/S1990793122010274.
9 O. A. Lessa, I. M. de Carvalho Tavares, L. O. Souza, L. G. P. Tienne, M. C. Dias, G. H. D. Tonoli, *et al.*, New biodegradable film produced from cocoa shell nanofibrils containing bioactive compounds, *J. Coat. Technol. Res.*, 2021, **18**, 1613–1624, DOI: 10.1007/s11998-021-00519-4.
10 S. A. Qamar, S. Piccolella, G. R. Ziegler, S. Pacifico and Y. Zhang, Functional bioplastic films from cocoa shell cellulose and natural waxes: Toward sustainable active packaging, *Food Packag Shelf Life*, 2025, **52**, 101595, DOI: 10.1016/j.fpsl.2025.101595.
11 F. Fetriyuna, M. Djali, Z. Rafi, D. A. Nurunnisa and R. C. Purwestri, Cocoa Bean Shells: A Potential Chocolate Replacement in Food, *Production*, 2025, **15**, 147–155, DOI: 10.18517/ijaseit.15.1.20270.
12 F. Lu, J. Rodriguez-Garcia, I. Van Damme, N. J. Westwood, L. Shaw, J. S. Robinson, *et al.*, Valorisation strategies for cocoa pod husk and its fractions, *Curr Opin Green Sustain Chem*, 2018, **14**, 80–88, DOI: 10.1016/j.cogsc.2018.07.007.
13 V. N. H. Vu, T. Q. Cao, T. T. H. Nguyen, L. T. N. Nguyen, P. H. Le and V. Nguyen, Extraction of Bioactive Compounds from Cocoa Pod Husk (Theobroma cacao L.) Using Deep Eutectic Solvent Assisted with Ultrasound, *Nat. Prod. Commun.*, 2025, **20**, 1934578X251333026, DOI: 10.1177/1934578X251333026.
14 E. Alvarez-Yanamango, D. Obregon and A. Ibañez, A Comprehensive Review of the Development of Green Extraction Methods and Encapsulation of Theobromine from Cocoa Bean Shells for Nutraceutical Applications, *Food Eng. Rev.*, 2025, **17**, 1083–1104, DOI: 10.1007/s12393-025-09425-6.
15 M. D. Esclapez, J. V. García-Pérez, A. Mulet and J. A. Cárcel, Ultrasound-Assisted Extraction of Natural Products, *Food Eng. Rev.*, 2011, **3**, 108–120, DOI: 10.1007/s12393-011-9036-6.
16 M. Mushtaq, Q. A. Amin, T. A. Wani, S. Z. Hussain, T. A. Bhat, S. Parveen, *et al.*, Cavitation-driven extraction: how ultrasound-induced acoustic cavitation maximizes bioactive compound recovery from S. costus roots, *Ultrason. Sonochem.*, 2025, **122**, 107643, DOI: 10.1016/j.ultsonch.2025.107643.
17 P. Vazquez-Roig and Y. Picó, Pressurized liquid extraction of organic contaminants in environmental and food samples, *TrAC, Trends Anal. Chem.*, 2015, **71**, 55–64, DOI: 10.1016/j.trac.2015.04.014.
18 S. G. Papadaki, K. E. Kyriakopoulou and M. K. Krokida, Life cycle analysis of microalgae extraction techniques, *Chem Eng Trans*, 2016, **52**, 1039–1044, DOI: 10.3303/CET1652174.
19 S. A. Siddiqui, A. Ali Redha, M. Salauddin, I. A. Harahap and H. P. V. Rupasinghe, Factors Affecting the Extraction of (Poly)Phenols from Natural Resources Using Deep Eutectic Solvents Combined with Ultrasound-Assisted Extraction, *Crit. Rev. Anal. Chem.*, 2025, **55**, 139–160, DOI: 10.1080/10408347.2023.2266846.
20 S. R. Shirsath, S. H. Sonawane and P. R. Gogate, Intensification of extraction of natural products using ultrasonic irradiations: A review of current status, *Chem. Eng. Process.*, 2012, **53**, 10–23, DOI: 10.1016/j.cep.2012.01.003.
21 F. Oyoun, A. Toncheva, L. C. Henríquez, R. Grougnet, F. Laoutid, N. Mignet, *et al.*, Deep Eutectic Solvents: An Eco-friendly Design for Drug Engineering, *ChemSusChem*, 2023, **16**, e202300669, DOI: 10.1002/cssc.202300669.
22 T. El Achkar, H. Greige-Gerges and S. Fourmentin, Basics and properties of deep eutectic solvents: a review, *Environ. Chem. Lett.*, 2021, **19**, 3397–3408, DOI: 10.1007/s10311-021-01225-8.
23 M. Ivanović, M. I. Razboršek and M. Kolar, Innovative Extraction Techniques Using Deep Eutectic Solvents and Analytical Methods for the Isolation and Characterization of Natural Bioactive Compounds from Plant Material, *Plants*, 2020, **9**, 1–29, DOI: 10.3390/plants9111428.
24 T. Swebocki, A. M. Kocot, K. Cieminska, C. Bortolus, J. Muchembled, M. S. Mechouche, *et al.*, Breaking through Microbial Defenses—Organic Acid-Based Deep Eutectic Solvents as a Neoteric Strategy in Bacterial Biofilms, Persister, and Fungal Control, *ACS Appl Bio Mater*, 2025, **8**, 8980–8990, DOI: 10.1021/acsabm.5c01159.
25 V. A. Tirado-Kulieva, M. Sánchez-Chero, M. Villegasyarlequé, G. F. V. Aguilar, G. Carrión-Barco, A. G. Y. Santa Cruz, *et al.*, An Overview on the Use of Response Surface Methodology to Model and Optimize Extraction Processes in the Food Industry, *Curr. Res. Nutr. Food Sci*, 2021, **9**, 745–754, DOI: 10.12944/CRNFSJ.9.3.03.
26 Q. Xia, C. Chen, Y. Yao, J. Li, S. He, Y. Zhou, *et al.*, A strong, biodegradable and recyclable lignocellulosic bioplastic, *Nat Sustainability*, 2021, **4**, 627–635, DOI: 10.1038/s41893-021-00702-w.
27 V. L. Singleton, R. Orthofer and R. M. Lamuela-Raventós, Analysis of total phenols and other oxidation substrates and antioxidants by means of folin-ciocalteu reagent, *Methods Enzymol.*, 1999, **299**, 152–178, DOI: 10.1016/S0076-6879(99)99017-1.
28 M. Blasa, M. Candiracci, A. Accorsi, M. P. Piacentini, M. C. Albertini and E. Piatti, Raw Millefiori honey is packed full of antioxidants, *Food Chem.*, 2006, **97**, 217–222, DOI: 10.1016/j.foodchem.2005.03.039.
29 B. Rodríguez-Martínez, P. Ferreira-Santos, I. M. Alfonso, S. Martínez, Z. Genisheva and B. Gullón, Deep Eutectic Solvents as a Green Tool for the Extraction of Bioactive

Phenolic Compounds from Avocado Peels, *Molecules*, 2022, **27**, 6646, DOI: 10.3390/molecules27196646.

30 Z. Shen, X. Ji, S. Yao, H. Zhang, L. Xiong, H. Li, *et al.*, Solid-liquid extraction of chlorogenic acid from Eucommia ulmoides Oliver leaves: Kinetic and mass transfer studies, *Ind. Crops Prod.*, 2023, **205**, 117544, DOI: 10.1016/j.indcrop.2023.117544.

31 N. Elboughdiri. *Effect of Time, Solvent-Solid Ratio, Ethanol Concentration and Temperature on Extraction Yield of Phenolic Compounds from Olive Leaves*. vol. 8. 2018. DOI: 10.48084/etasr.1983.

32 G. H. Huynh, H. Van Pham and H. V. Hong Nguyen, Effects of enzymatic and ultrasonic-assisted extraction of bioactive compounds from cocoa bean shells, *Food Meas. Charact*, 2023, **17**, 4650–4660, DOI: 10.1007/s11694-023-01986-6.

33 O. R. Alara, N. H. Abdurahman and C. I. Ukaegbu, Extraction of phenolic compounds: A review, *Curr Res Food Sci*, 2021, **4**, 200–214, DOI: 10.1016/j.crfs.2021.03.011.

34 F. Gabriele, M. Chiarini, R. Germani and N. Spreti, Understanding the role of temperature in structural changes of choline chloride/glycols deep eutectic solvents, *J. Mol. Liq.*, 2023, **385**, 122332, DOI: 10.1016/j.molliq.2023.122332.

35 F. Lin, Z. Zuo, B. Cao, H. Wang, L. Lu, X. Lu, *et al.*, A Comprehensive Study of Density, Viscosity, and Electrical Conductivity of Choline Halide-Based Eutectic Solvents in H2O, *J. Chem. Eng. Data*, 2024, **69**, 4362–4376, DOI: 10.1021/ACS.JCED.4C00218.

36 J. K. U. Ling and K. Hadinoto, Deep Eutectic Solvent as Green Solvent in Extraction of Biological Macromolecules: A Review, *Int. J. Mol. Sci.*, 2022, **23**, 3381, DOI: 10.3390/IJMS23063381.

37 W. Tang, G. Li, B. Chen, T. Zhu and K. H. Row, Evaluating ternary deep eutectic solvents as novel media for extraction of flavonoids from Ginkgo biloba, *Sep. Sci. Technol. (Philadelphia, PA, U. S.)*, 2017, **52**, 91–99, DOI: 10.1080/01496395.2016.1247864.

38 M. Irsal, M. Yusuf, M. T. Al Hayah, A. A. Ma'Ruf, M. R. Mahmud and S. N. Rahayu, Ultrasonic - Assisted Extraction and Microencapsulation of Bioactive Compound From Pigeon Pea Seed, *Bull. Pharm. Sci., Assiut Univ.*, 2023, **46**, 51–62, DOI: 10.21608/BFSA.2023.300760.

39 N. L. Joey, N. A. Ismail, A. M. Ahmad Mokhtar and M. S. Che Zain, Integrated ultrasonic–natural deep eutectic solvent-assisted extraction for standardizing polyphenol-enriched extract from cocoa (Theobroma Cacao L.) rind with enhanced antioxidant properties, *Food Meas. Charact*, 2025, **20**, 357–375, DOI: 10.1007/S11694-025-03673-0plan.

40 E. Benítez-Correa, J. M. Bastías-Montes, S. Acuña-Nelson and O. Muñoz-Fariña, Effect of choline chloride-based deep eutectic solvents on polyphenols extraction from cocoa (Theobroma cacao L.) bean shells and antioxidant activity of extracts, *Curr Res Food Sci*, 2023, **7**, 100614, DOI: 10.1016/j.crfs.2023.100614.

41 Q. Li, Y. Dong, K. D. Hammond and C. Wan, Revealing the role of hydrogen bonding interactions and supramolecular complexes in lignin dissolution by deep eutectic solvents, *J. Mol. Liq.*, 2021, **344**, 117779, DOI: 10.1016/j.molliq.2021.117779.

42 F. Ramos-Escudero, A. Rojas-García, M. de la L. Cádiz-Gurrea and A. Segura-Carretero, High potential extracts from cocoa byproducts through sonotrode optimal extraction and a comprehensive characterization, *Ultrason. Sonochem.*, 2024, **106**, 106887, DOI: 10.1016/j.ultsonch.2024.106887.

43 X. Pan, Y. Liu, Z. Ma, Y. Qin, X. Lu, X. Feng, *et al.*, Molecular insight into the mechanism of lignin dissolution in acid choline chloride–Based deep eutectic solvents, *J. Mol. Liq.*, 2024, **406**, 125123, DOI: 10.1016/j.molliq.2024.125123.

44 P. Larkin. *Infrared and Raman Spectroscopy: Principles and Spectral Interpretation*. 2011. DOI: 10.1016/C2010-0-68479-3.

45 M. Irsal, Y. Kusumastuti, T. Ariyanto, N. Rofiqoh and E. Putri, Kinetic study of bioactive compound extraction from cacao shell waste by conventional and deep eutectic solvent, *Commun. Sci. Technol*, 2025, **10**, 117–124, DOI: 10.21924/cst.10.1.2025.1606.

46 C. Nursiah, H. Desvita, E. Elviani, N. Farida, A. Muslim, C. M. Rosnelly, *et al.*, Adsorbent Characterization from Cocoa Shell Pyrolysis (Theobroma cacao L) and its Application in Mercury Ion Reduction, *J. Ecol. Eng.*, 2023, **24**, 366–375, DOI: 10.12911/22998993/163167.

47 X. Wang, W. Jia, G. Lai, L. Wang, M. del Mar Contreras and D. Yang, Extraction for profiling free and bound phenolic compounds in tea seed oil by deep eutectic solvents, *J. Food Sci.*, 2020, **85**, 1450–1461, DOI: 10.1111/1750-3841.15019.

48 T. K. Patle, K. Shrivas, R. Kurrey, S. Upadhyay, R. Jangde and R. Chauhan, Phytochemical screening and determination of phenolics and flavonoids in Dillenia pentagyna using UV–vis and FTIR spectroscopy, *Spectrochim Acta A Mol Biomol Spectrosc*, 2020, **242**, 118717, DOI: 10.1016/j.saa.2020.118717.

49 N. Giummarella and M. Lawoko, Structural Insights on Recalcitrance during Hydrothermal Hemicellulose Extraction from Wood, *ACS Sustain. Chem. Eng.*, 2017, **5**, 5156–5165, DOI: 10.1021/acssuschemeng.7b00511.

50 X. Liu, C. M. G. C. Renard, S. Bureau and C. Le Bourvellec, Revisiting the contribution of ATR-FTIR spectroscopy to characterize plant cell wall polysaccharides, *Carbohydr. Polym.*, 2021, **262**, 117935, DOI: 10.1016/J.CARBPOL.2021.117935.

51 T. Hong, J. Y. Yin, S. P. Nie and M. Y. Xie, Applications of infrared spectroscopy in polysaccharide structural analysis: Progress, challenge and perspective, *Food Chem X*, 2021, **12**, 100168, DOI: 10.1016/j.fochx.2021.100168.

52 L. Valadez-Carmona, C. P. Plazola-Jacinto, M. Hernández-Ortega, M. D. Hernández-Navarro, F. Villarreal, H. Necoechea-Mondragón, *et al.*, Effects of microwaves, hot air and freeze-drying on the phenolic compounds, antioxidant capacity, enzyme activity and microstructure of cacao pod husks (Theobroma cacao L.), *Innovative Food Sci. Emerging Technol.*, 2017, **41**, 378–386, DOI: 10.1016/j.ifset.2017.04.012.

53 T. Belwal, C. Cravotto, S. Ramola, M. Thakur, F. Chemat and G. Cravotto, Bioactive Compounds from Cocoa Husk:

Extraction, Analysis and Applications in Food Production Chain, *Foods*, 2022, **11**, 2022–11, DOI: 10.3390/foods11060798.

54 M. Krysa, M. Szymańska-Chargot and A. Zdunek, FT-IR and FT-Raman fingerprints of flavonoids – A review, *Food Chem.*, 2022, **393**, 133430, DOI: 10.1016/j.foodchem.2022.133430.

55 D. Patabang, S. J. T. Basri and K. Seleng, Effect of cocoa pods husk blending on combustion characteristics of the low-rank coal analyzed in TGA, *Int. J. Coal Prep. Util.*, 2024, **44**, 605–613, DOI: 10.1080/19392699.2023.2212597.

56 Z. Chen, M. Hu, X. Zhu, D. Guo, S. Liu, Z. Hu, *et al.*, Characteristics and kinetic study on pyrolysis of five lignocellulosic biomass *via* thermogravimetric analysis, *Bioresour. Technol.*, 2015, **192**, 441–450, DOI: 10.1016/j.biortech.2015.05.062.

57 W. H. Chen, C. F. Eng, Y. Y. Lin and Q. V. Bach, Independent parallel pyrolysis kinetics of cellulose, hemicelluloses and lignin at various heating rates analyzed by evolutionary computation, *Energy Convers Manag*, 2020, **221**, 113165, DOI: 10.1016/j.enconman.2020.113165.

58 L. O. Souza, O. A. Lessa, M. C. Dias, G. H. D. Tonoli, D. V. B. Rezende, M. A. Martins, *et al.*, Study of morphological properties and rheological parameters of cellulose nanofibrils of cocoa shell (Theobroma cacao L.), *Carbohydr. Polym.*, 2019, **214**, 152–158, DOI: 10.1016/j.carbpol.2019.03.037.

59 A. Younes, M. Li and S. Karboune, Cocoa bean shells: a review into the chemical profile, the bioactivity and the biotransformation to enhance their potential applications in foods, *Crit Rev Food Sci Nutr*, 2023, **63**, 9111–9135, DOI: 10.1080/10408398.2022.2065659.

60 D. Smink, S. R. A. Kersten and B. Schuur, Process development for biomass delignification using deep eutectic solvents. Conceptual design supported by experiments, *Chem. Eng. Res. Des.*, 2020, **164**, 86–101, DOI: 10.1016/j.cherd.2020.09.018.

61 E. K. New, T. Y. Wu, C. B. Tien Loong Lee, Z. Y. Poon, Y. L. Loow, L. Y. Wei Foo, *et al.*, Potential use of pure and diluted choline chloride-based deep eutectic solvent in delignification of oil palm fronds, *Process Saf. Environ. Prot.*, 2019, **123**, 190–198, DOI: 10.1016/j.psep.2018.11.015.

62 Z. K. Wang, S. Hong, J. L. Wen, C. Y. Ma, L. Tang, H. Jiang, *et al.*, Lewis Acid-Facilitated Deep Eutectic Solvent (DES) Pretreatment for Producing High-Purity and Antioxidative Lignin, *ACS Sustain. Chem. Eng.*, 2020, **8**, 1050–1057, DOI: 10.1021/acssuschemeng.9b05846.

63 K. M. Lee, J. D. Quek, W. Y. Tey, S. Lim, H. S. Kang, L. K. Quen, *et al.*, Biomass valorization by integrating ultrasonication and deep eutectic solvents: Delignification, cellulose digestibility and solvent reuse, *Biochem. Eng. J.*, 2022, **187**, 108587, DOI: 10.1016/j.bej.2022.108587.

64 X. Chen, W. Lan and J. Xie, Natural phenolic compounds: Antimicrobial properties, antimicrobial mechanisms, and potential utilization in the preservation of aquatic products, *Food Chem.*, 2024, **440**, 138198, DOI: 10.1016/j.foodchem.2023.138198.

65 F. R. Dewi, S. M. Powell, R. A. Stanley, S. Gam, P. Kalita, B. Gogoi, *et al.*, The antimicrobial effectiveness of cacao shell and cacao husk combination on inhibition of pathogenic bacteria in food products, *IOP Conf Ser Earth Environ Sci*, 2020, **443**, 012077, DOI: 10.1088/1755-1315/443/1/012077.

66 M. Rahban, S. Zolghadri, N. Salehi, F. Ahmad, T. Haertlé, N. Rezaei-Ghaleh, *et al.*, Thermal stability enhancement: Fundamental concepts of protein engineering strategies to manipulate the flexible structure, *Int. J. Biol. Macromol.*, 2022, **214**, 642–654, DOI: 10.1016/j.ijbiomac.2022.06.154.

67 M. M. Huang, C. L. Yiin, S. S. Mun Lock, B. L. Fui Chin, I. Othman, N. S. binti Ahmad Zauzi, *et al.*, Natural deep eutectic solvents (NADES) for sustainable extraction of bioactive compounds from medicinal plants: Recent advances, challenges, and future directions, *J. Mol. Liq.*, 2025, **425**, 127202, DOI: 10.1016/j.molliq.2025.127202.

68 F. J. Álvarez-Martínez, E. Barrajón-Catalán, J. A. Encinar, J. C. Rodríguez-Díaz and V. Micol, Antimicrobial Capacity of Plant Polyphenols against Gram-positive Bacteria: A Comprehensive Review, *Curr. Med. Chem.*, 2018, **27**, 2576–2606, DOI: 10.2174/0929867325666181008115650.

69 M. Winterhalter and M. Ceccarelli, Physical methods to quantify small antibiotic molecules uptake into Gram-negative bacteria, *Eur. J. Pharm. Biopharm.*, 2015, **95**, 63–67, DOI: 10.1016/j.ejpb.2015.05.006.

70 H. Qin, X. Hu, J. Wang, H. Cheng, L. Chen and Z. Qi, Overview of acidic deep eutectic solvents on synthesis, properties and applications, *Green Energy Environ.*, 2020, **5**, 8–21, DOI: 10.1016/j.gee.2019.03.002.